

Dynamics of mass asymmetry in nuclear molecular systems

G.G. Adamian^a, A. Andreev^{a,b}, N.V. Antonenko^{a,b}, R.V. Jolos^{a,b},
S.P. Ivanova^a, Yu.V. Palchikov^a, W. Scheid^{b,*}, and T.M. Schneidman^a

^aJoint Institute for Nuclear Research,
141980 Dubna (Moscow Region), Russia,

^bInstitut für Theoretische Physik der Universität,
35392 Giessen, Germany,

*e-mail: werner.scheid@theo.physik.uni-giessen.de

Recibido el 27 de enero de 2006; aceptado el 10 de mayo de 2006

The dinuclear system concept assumes two touching nuclei which can exchange nucleons by transfer. This concept can be applied to nuclear structure, to fusion reactions leading to superheavy nuclei and to multi-nucleon transfer.

Keywords: Dinuclear system; superdeformed states; fusion; superheavy nuclei; quasifission.

El concepto de un sistema dinuclear supone dos nucleos en contacto que pueden intercambiar nucleones entre ellos. Posibles aplicaciones de este modelo se encuentran en la estructura nuclear, reacciones de fusión para crear núcleos superpesados y la transferencia de varios nucleones.

Descriptores: Sistema dinuclear; estados superdeformados; fusión, núcleos superpesados; cuasifusión.

PACS: 25.70.Ji; 24.10.-i; 21.60.Ev; 21.60.Gx

1. Introduction

A nuclear molecule or a dinuclear system (DNS) is a configuration of two touching nuclei (clusters) which keep their individuality. Such a system has two main degrees of freedom which govern its dynamics: (1) the relative motion between the nuclei describing the decay of the dinuclear system which is called quasifission and (2) the transfer of nucleons between the nuclei. The latter process changes the mass and charge asymmetries which are defined by the coordinates

$$\eta = \frac{A_1 - A_2}{A_1 + A_2} \quad \text{and} \quad \eta_Z = \frac{Z_1 - Z_2}{Z_1 + Z_2}. \quad (1)$$

These coordinates can be assumed as continuous or discrete quantities. For $\eta = \eta_Z = 0$ we have a symmetric clusterization with two equal nuclei, and if η approaches the values ± 1 or if A_1 or A_2 is equal to zero, a fused system has been formed. The importance of the mass (charge) coordinate was pointed out by Fink *et al.* [1] and by V.V. Volkov [2].

This article gives a short and concise review on newer applications of the DNS model achieved in the last two years which summarizes the important role of the mass asymmetry degree of freedom for various nuclear structure and reaction phenomena. In the following we consider nuclear structure phenomena like normal- and superdeformed bands, the fusion dynamics in producing superheavy nuclei, and the quasifission of the dinuclear system. Besides this review the article contains a thorough comparison of adiabatic and diabatic potentials used to describe the production of superheavy nuclei and presents new transfer cross sections for the production of heavier nuclei in the reaction of $^{76}\text{Ge} + ^{208}\text{Pb}$ obtained with master equations.

2. Dinuclear configuration

The dinuclear configuration describes quadrupole- and octupole-like deformations related with normal, super- and hyperdeformed states. To demonstrate the deformation of the dinuclear configuration, we calculated [3] the mass and charge multipole moments of a nucleus described by a dinuclear configuration with a (mass and charge) density $\varrho(\mathbf{r}) = \varrho_1(\mathbf{r}_1) + \varrho_2(\mathbf{r}_2)$, where ϱ_i ($i = 1, 2$) is the density of the individual nucleus i . Since the nuclei only touch each other, the antisymmetrization between the nuclei does not play a decisive role. The moments are compared with those of an axially deformed nucleus by use of a shape expansion with multipole deformation parameters $\beta_\lambda = \beta_0, \beta_1, \beta_2, \beta_3 \dots$. Then one obtains these parameters β_λ as functions of η or η_Z . For spherical clusters they are nearly independent of A . Realistic clusters yield a specific dependence on the surface thickness, the radius parameters and their deformations [3].

The dinuclear system model can be applied in the range of $\eta = 0 - 0.3$ to hyperdeformed (HD) states (nuclei with large quadrupole deformation), in the range of $\eta = 0.6 - 0.9$ to superdeformed (SD) states (similar quadrupole and octupole deformations) and around $\eta \approx 1$ to the parity splitting of bands (linear increase of deformations). As example let us discuss the ^{152}Dy system [3]. The potential energy of the DNS as a function of η shows significant minima for $\eta = 0.34$ ($^{50}\text{Ti} + ^{102}\text{Ru}$), $\eta = 0.66$ ($^{26}\text{Mg} + ^{126}\text{Xe}$) and $\eta = 0.71$ ($^{22}\text{Ne} + ^{130}\text{Ba}$). The DNS $^{50}\text{Ti} + ^{102}\text{Ru}$ is compatible with HD properties, the dinuclear systems $^{26}\text{Mg} + ^{126}\text{Xe}$ and $^{22}\text{Ne} + ^{130}\text{Ba}$ have SD properties. For $^{26}\text{Mg} + ^{126}\text{Xe}$ we calculated a moment of inertia of $J=104 \hbar^2/\text{MeV}$ and an electric quadrupole moment of $Q_2=24 \text{ eb}$ in comparison with

the experimental values of SD states with $J=(85\pm 3)\hbar^2/\text{MeV}$ and $Q_2=(18\pm 3)\text{ eb}$ (see [4]).

3. Normal- and superdeformed bands

The DNS model can be used to describe the normaldeformed (ND) and superdeformed bands of various nuclei. We applied this model to the structure of ^{60}Zn [5] and of $^{190,192,194}\text{Hg}$ and $^{192,194,196}\text{Pb}$ [6].

The ^{60}Zn nucleus has a threshold of 2.7 MeV above ground state for its decay into $^{56}\text{Ni} + \alpha$. Therefore, we can assume that the ground state band contains an α -component. Further thresholds are positioned at 10.8 and 11.2 MeV above the ground state for the decays into $^{52}\text{Fe} + ^8\text{Be}$ and $^{48}\text{Cr} + ^{12}\text{C}$, respectively. The extrapolated band head of the SD band has an energy of 7.5 MeV and a moment of inertia of $(692\text{-}795)M\text{ fm}^2$ in comparison with the moment of inertia of the $^{52}\text{Fe} + ^8\text{Be}$ system of $750 M\text{ fm}^2$ where M is the nucleon mass. Hence, the SD band of ^{60}Zn contains a prominent ^8Be component.

The observed strong collective dipole transitions between the excited SD band and the lowest-energy SD band in ^{150}Gd , ^{152}Dy , $^{190,194}\text{Hg}$, $^{196,198}\text{Pb}$ and between the SD and ND bands in ^{194}Hg and ^{194}Pb indicate a decay out of pronounced octupole deformed states [7]. The measured properties of the excited SD bands in ^{152}Dy and $^{190,192,194}\text{Hg}$ have been interpreted in terms of rotational bands built on collective octupole vibrations. Configurations with large quadrupole and octupole deformation parameters and low-lying collective negative parity states are strongly related to a clustering describable with heavy and light clusters within the DNS model.

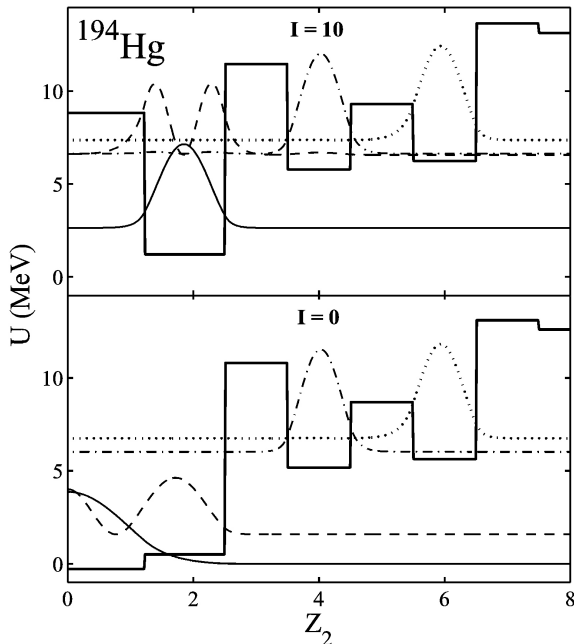


FIGURE 1. Potential energy (histogram) U of ^{194}Hg for the spins $I = 0$ and 10 . The curves are the absolute squares of the wave functions of the ground (solid) and first excited (dashed) ND bands and ground (dashed-dotted) and first excited (dotted) SD bands.

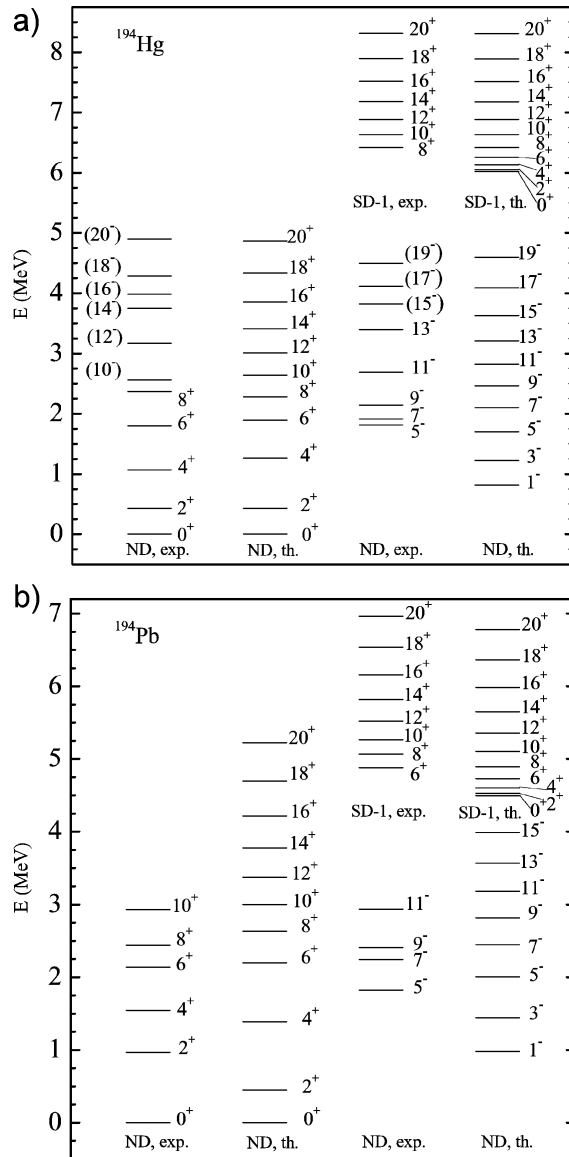


FIGURE 2. Calculated and experimental levels of the ground state and superdeformed bands of ^{194}Hg (l.h.s.) and ^{194}Pb (r.h.s.). Experimental data are taken from [10] and [11].

The cluster picture of the above mentioned ND and SD bands can be consistently treated by assuming a collective dynamics in the mass or charge asymmetry coordinate η or η_Z , respectively. To achieve this aim, we formulate a conventional collective Schrödinger equation in η_Z (or η) [5]:

$$\left(-\frac{\hbar^2}{2} \frac{d}{d\eta_Z} \frac{1}{B_{\eta_Z}} \frac{d}{d\eta_Z} + U(\eta_Z, I) \right) \psi_n(\eta_Z, I) = E_n(I) \psi_n(\eta_Z, I). \quad (2)$$

In Fig. 1 we show the calculated potential U of ^{194}Hg as a function of the charge number Z_2 of the lighter cluster for two nuclear spins $I = 0$ and 10 . The potential has minima for α -type clusterizations, namely for $Z_2 = 2, 4, 6, 8, \dots$. In addition Figure 1 presents the probability $|\psi_n(\eta_Z, I)|^2$ expressed with the intrinsic wave functions of the ND and SD states.

This probability is peaked around the minima of the potential indicating a corresponding cluster structure of the states. In Fig. 2 we show as example the calculated level spectra of ^{194}Hg and ^{194}Pb in comparison with the experimental data. We note that the shift of the negative parity states is reproducible with the dynamics in η_Z and is related to the properties of the octupole degree of freedom [8, 9]. Also electromagnetic transition probabilities can be evaluated [5, 6] with the intrinsic wave functions which agree well with the experimental data.

4. Dinuclear dynamics in the fusion process

Heavy and superheavy nuclei can be produced by fusion reactions with heavy ions. We discriminate Pb or Bi based or cold fusion reactions, *e.g.* $^{70}\text{Zn} + ^{208}\text{Pb} \rightarrow ^{278}112 \rightarrow ^{277}112 + n$ with an evaporation residue cross section of $\sigma = 1$ pb and an excitation energy of the $^{278}112$ compound nucleus of about 11 MeV [12], and actinide based or hot fusion reactions, *e.g.* $^{48}\text{Ca} + ^{244}\text{Pu} \rightarrow ^{288}114 + 4n$, with the emission of more neutrons [13]. The cross sections are small because of a strong competition between complete fusion and quasifission and small survival probabilities of the excited compound nucleus.

4.1. Models for production of superheavy nuclei

The models for the production of superheavy nuclei can be discriminated by the dynamics in the most important collective degrees of freedom of the system, *i.e.* the relative and mass asymmetry motions, and depend sensitively whether adiabatic or diabatic potentials in the internuclear coordinate R are assumed. The potentials are calculated by the Strutinsky method using the two-center shell model or by applying an experimental-theoretical method with experimental binding energies of the fragments and an internuclear folding potential, *e.g.* that of Migdal [14]. In both cases the potentials effectively include the effects of the Pauli principle.

- a) *Models using adiabatic potentials:* These models (see *e.g.* [15]) minimize the potential energy. In that case the nuclei first change their mass asymmetry in the direction to more symmetric clusters and then they fuse together by crossing a smaller fusion barrier in the relative coordinate around $\eta = 0$. The models tend to give large probabilities for fusion if similar target and projectile nuclei are taken which contradicts the exponential falling-off of the evaporation residue cross section with increasing projectile nuclei in Pb-based reactions.
- b) *Dinuclear system concept:* The fusion proceeds by a transfer of nucleons between the nuclei in a touching configuration, *i.e.* in the dinuclear configuration. Here, mainly a dynamics in the mass asymmetry degree of freedom occurs. The potential is of diabatic type with a minimum in the touching range and a repulsive part

towards smaller internuclear distances prohibiting the dinuclear system to amalgamate to the compound nucleus in the relative coordinate. Such a potential can be achieved with a diabatic two-center shell model [16] and can also be justified with structure calculations based on group theoretical methods [17] which explicitly take into account the Pauli principle.

4.2. Evaporation residue cross section

The cross section for the production of superheavy nuclei can be written [18]

$$\sigma_{ER}(E_{c.m.}) = \sum_{J=0}^{J_{max}} \sigma_{cap}(E_{c.m.}, J) P_{CN}(E_{c.m.}, J) W_{sur}(E_{c.m.}, J). \quad (3)$$

The three factors are the capture cross section, the probability for complete fusion and the survival probability. The maximal contributing angular momentum J_{max} is of the order of 10 - 20. The capture cross section σ_{cap} describes the formation of the dinuclear system at the initial stage of the reaction when the kinetic energy of the relative motion is transferred into potential and excitation energies. The DNS can decay by crossing the quasifission barrier B_{qf} which is of the order of 0.5 - 5 MeV.

After its formation the DNS evolves in the mass asymmetry coordinate. The center of the mass distribution moves towards more symmetric fragmentations and its width is broadened by diffusion processes. The part of the distribution, which crosses the inner fusion barrier B_{fus}^* of the driving potential $U(\eta)$, yields the probability P_{CN} for complete fusion. The DNS can also decay by quasifission during its evolution. Therefore, the fusion probability P_{CN} and the mass and charge distributions of the quasifission have to be treated simultaneously. The fusion probability can be quantitatively estimated with the Kramers formula [19] and results as $P_{CN} \sim \exp(-(B_{fus}^* - \min[B_{qf}, B_{sym}])/T)$ where the temperature T is related to the excitation energy of the DNS, and B_{sym} is the barrier in η to more symmetric configurations. B_{sym} is 4-5 MeV ($> B_{qf}$) in cold fusion reactions and 0.5-1.5 MeV ($< B_{qf}$) in hot fusion reactions. Since the inner fusion barrier increases with decreasing mass asymmetry, we find an exponential depression of the fusion probability towards symmetric projectile and target combinations in lead based reactions [18]. In hot fusion reactions with ^{48}Ca projectiles, P_{CN} drops slightly down with increasing mass and charge of the target nucleus [20]. These systems run easier towards symmetric fragmentations and undergo quasifission there.

The excited compound nucleus decays by fission and emits neutrons besides other negligible decays. The probability to reach the ground state of the superheavy nucleus by neutron emission is denoted as survival probability W_{sur} . In the case of the one-neutron emission in Pb-based reactions the survival probability is roughly the ratio Γ_n/Γ_f of the

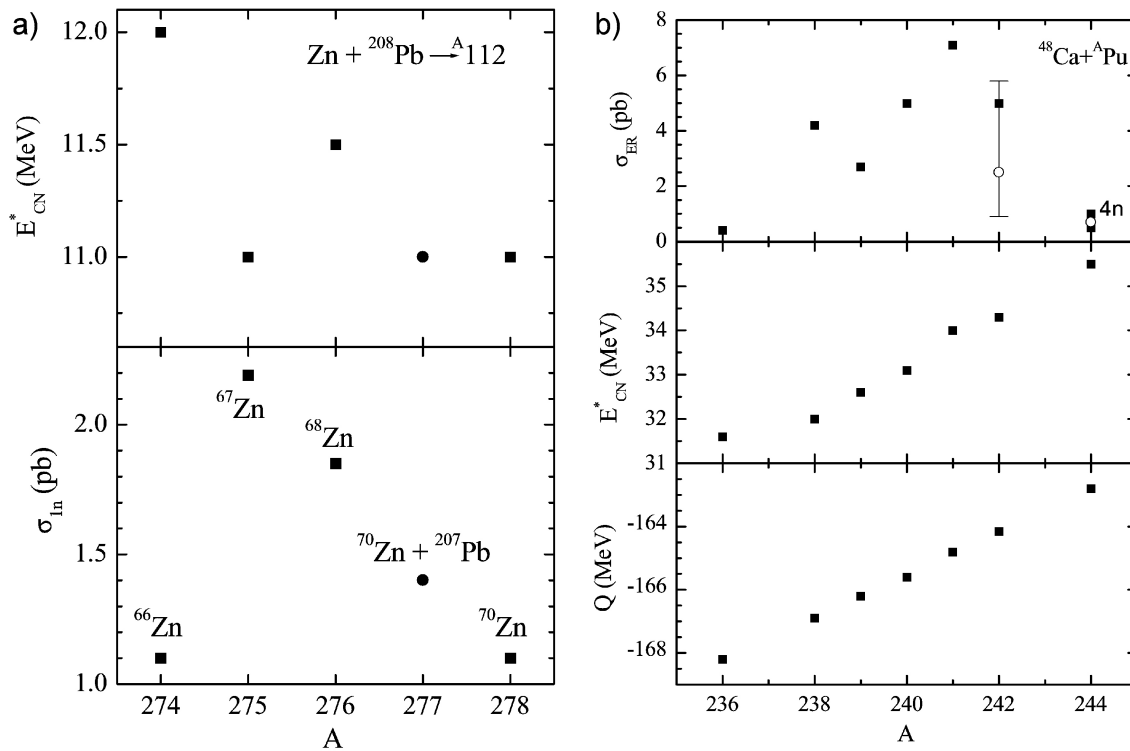


FIGURE 3. Excitation energy E_{CN}^* , evaporation residue cross sections σ_{1n} , σ_{3n} , σ_{4n} , and Q -value for $Zn + {}^{208}Pb \rightarrow {}^A112$ (l.h.s.) and ${}^{48}Ca + {}^A Pu$ (r.h.s.). The experimental data are from Ref. 13.

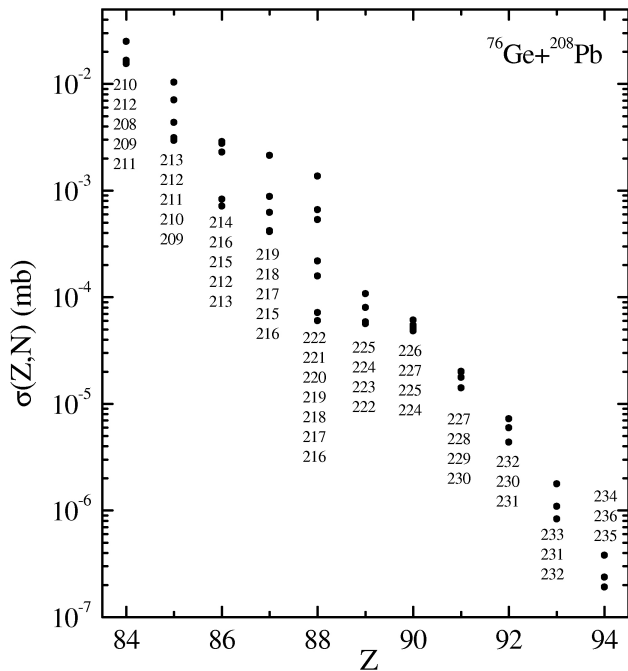


FIGURE 4. Calculated production cross section in the reaction ${}^{76}Ge + {}^{208}Pb$ as a function of Z and A of the heavier fragment.

widths for neutron emission and for fission because of $\Gamma_f \gg \Gamma_n$. The survival probability depends sensitively on the nuclear structure properties of the superheavy elements as level density, fission barriers and deformation [21].

With the DNS concept we reproduced the measured evaporation residue cross sections of the Pb- and actinide-based reactions with a precision of a factor of two (see Refs. 18 and 20). This concept also yields the excitation energies of the superheavy compound nuclei at the optimal bombarding energies (largest production cross sections) in agreement with the experimental data.

4.3. Isotopic dependence of production cross section

An opinion is that the production cross section of isotopic superheavy nuclei is increasing with the neutron number. For example, the evaporation residue cross section of Ds ($Z = 110$) increases with the neutron number. The reactions ${}^{62}Ni + {}^{208}Pb \rightarrow {}^{269}Ds + n$ and ${}^{64}Ni + {}^{208}Pb \rightarrow {}^{271}Ds + n$ have cross sections of 3.5 and 15 pb, respectively [12]. This opinion can not be generalized. When the neutron number of the projectile is increasing, the dinuclear fragmentation gets more symmetrically and the fusion probability decreases if the more symmetric DNS does not consist of more stable nuclei. Also the survival probability is of importance. For compound nuclei with closed neutron shells the survival probability is larger. Hence, the product of P_{CN} and W_{sur} determines whether the production cross section increases or decreases with increasing neutron number. Figure 3 shows examples for cold and hot fusion reactions [20]. These calculations are very valuable and necessary for an adequate choice of projectile and target nuclei in experiment.

5. Quasifission as signature for mass transfer

The process of quasifission is the decay of the DNS. Since quasifission leads to a large quantity of observable data like mass and charge distributions, distributions of total kinetic energies (TKE), variances of total kinetic energies and neutron multiplicities, a comparison of the theoretical description with experimental data provides sensitive information about the applicability and correctness of the used model. For this reason we studied the dynamics of mass and charge transfer and the succeeding quasifission with master equations [22]. At the starting point we consider the shell model Hamiltonian of all dinuclear fragmentations of the nucleons [23]. This Hamiltonian can be used to derive master equations for the probability $P_{Z,N}(t)$ to find the dinuclear system in a fragmentation with $Z_1 = Z$, $N_1 = N$ and $Z_2 = Z_{tot} - Z$, $N_2 = N_{tot} - N$. The master equations are

$$\begin{aligned} \frac{d}{dt} P_{Z,N}(t) &= \Delta_{Z+1,N}^{(-,0)} P_{Z+1,N}(t) + \Delta_{Z-1,N}^{(+,0)} P_{Z-1,N}(t) \\ &+ \Delta_{Z,N+1}^{(0,-)} P_{Z,N+1}(t) + \Delta_{Z,N-1}^{(0,+)} P_{Z,N-1}(t) \\ &- \left(\Delta_{Z,N}^{(-,0)} + \Delta_{Z,N}^{(+,0)} + \Delta_{Z,N}^{(0,-)} + \Delta_{Z,N}^{(0,+)} \right) P_{Z,N}(t) \\ &- \Lambda_{Z,N}^{qf} P_{Z,N}(t). \end{aligned} \quad (4)$$

The one-proton and one-neutron transfer rates $\Delta^{(\dots)}$ depend on the single-particle energies and the temperature of the DNS where the occupation of the single-particle states is taken into account by a Fermi distribution. The simultaneous transfer of more nucleons is neglected. The quantity $\Lambda_{Z,N}^{qf}$ is the rate for quasifission in the coordinate R and is calculated with the Kramers formula [19]. This rate causes a loss of the total probability $\sum P_{Z,N}(t) \leq 1$. Then the mass yield

is obtained as

$$Y(A_1) = \sum_{Z_1} \int_0^{t_0} \Lambda_{Z_1, A_1 - Z_1}^{qf} P_{Z_1, A_1 - Z_1}(t) dt, \quad (5)$$

where $t_0 \approx (3 - 5) \times 10^{-20}$ s is the reaction time. The DNS dynamics was also studied by Li *et al.* [24] with similar master equations.

- a) *Results for quasifission* [22]: We calculated quasifission distributions, TKEs, variances of TKE and neutron multiplicities for cold and hot fusion reactions and found satisfying agreement with the experimental data of Itkis *et al.* [25]. For heavier systems, *e.g.* $^{48}\text{Ca} + ^{248}\text{Cm}$, the contribution of fission products to the mass distribution can be neglected since the probability for forming a compound nucleus is very small.
- b) *New calculations of production cross sections for asymmetric systems*: The master equations give also probabilities for more asymmetric systems than the initial one. In Fig. 4 we present production (transfer) cross sections for asymmetric fragmentations in the reaction $^{76}\text{Ge} + ^{208}\text{Pb}$ [26]. The measurement of these observable cross sections would be an unique proof for the fusion dynamics in the dinuclear system concept.

Acknowledgements

We thank DFG (Bonn), VW-Stiftung (Hannover) and RFBR (Moscow) for supporting this work. We thank Prof. Junqing Li (Lanzhou), Prof. Enguang Zhao (Beijing) and Prof. Nikolay Minkov (Sofia) for valuable discussions.

-
1. H.J. Fink *et al.*, *Z. f. Physik* **268** (1974) 321.
 2. V.V. Volkov, *Izv. AN SSSR ser. fiz.* **50** (1986) 1879.
 3. T.M. Shneidman *et al.*, *Nucl. Phys. A* **671** (2000) 119.
 4. S. Aberg, *Nucl. Phys. A* **557** (1993) 17.
 5. G.G. Adamian *et al.*, *Phys. Rev. C* **67** (2003) 054303.
 6. G.G. Adamian *et al.*, *Phys. Rev. C* **69** (2004) 054310.
 7. T. Nakatsukasa *et al.*, *Phys. Rev. C* **53** (1996) 2213.
 8. T.M. Shneidman *et al.*, *Phys. Lett. B* **526** (2002) 322.
 9. T.M. Shneidman *et al.*, *Phys. Rev. C* **67** (2003) 014313.
 10. T.L. Khoo *et al.*, *Phys. Rev. Lett.* **76** (1996) 1583; G. Hackman *et al.*, *ibid.* **79** (1997) 4100.
 11. A. Lopez-Martens *et al.*, *Phys. Lett. B* **380** (1996) 18; J.R. Hughes *et al.*, *Phys. Rev. C* **50** (1994) R1265; K. Hauschild *et al.*, *ibid.* **55** (1997) 2819.
 12. S. Hofmann and G. Münzenberg, *Rev. Mod. Phys.* **72** (2000) 733; S. Hofmann, *Rep. Prog. Phys.* **61** (1998) 636.
 13. Yu. Ts. Oganessian *et al.*, *Eur. Phys. J. A* **13** (2002) 135; **15** (2002) 201.
 14. A.B. Migdal, *Theory of Finite Fermi Systems and Application to Atomic Nuclei* (Nauka, Moscow, 1982); G.G. Adamian *et al.*, *Int. J. Mod. Phys. E* **5** (1996) 191.
 15. Y. Aritomo and M. Ohta, *Nucl. Phys. A* **744** (2004) 3.
 16. A. Diaz-Torres *et al.*, *Phys. Lett. B* **481** (2000) 228.
 17. G. G. Adamian *et al.*, *Phys. Lett. B* **451** (1999) 289.
 18. G. G. Adamian *et al.*, *Nucl. Phys. A* **633** (1998) 409; *ibid.* **678** (2000) 24.
 19. H.A. Weidenmüller and Jing-Shang Zhang, *J. Stat. Phys.* **34** (1984) 191.
 20. G.G. Adamian *et al.*, *Phys. Rev. C* **69** (2004) 011601 and 014607.
 21. A.S. Zubov *et al.*, *Eur. Phys. J. A* **23** (2005) 249.
 22. G.G. Adamian *et al.*, *Phys. Rev. C* **68** (2003) 034601.
 23. N.V. Antonenko and R.V. Jolos, *Z. Phys. A* **338** (1991) 423.

24. W. Li *et al.*, *Europhys. Lett.* **64** (2003) 750.
25. M.G. Itkis *et al.*, *Proceedings of the Carpathian Summer School of Physics 2005, Exotic Nuclei and Nuclear/Particle Astro-*
- physics*, Mamaia (Romania), (World Scientific, 2006).
26. G.G. Adamian and N.V. Antonenko, *Phys. Rev. C* **72** (2005) 064617.